GABA from vasopressin neurons regulates the time at which suprachiasmatic nucleus molecular clocks enable circadian behavior

Takashi Maejima[a], Yusuke Tsuno[a], Shota Miyazaki[b], Yousuke Tsuneoka[c], Emi Hasegawa[a,1], Md Tarikul Islam[a], Ryosuke Enoki[d,e], Takahiro J. Nakamura[b], and Michihiro Mieda[a,2]

[a]Department of Integrative Neurophysiology, Graduate School of Medical Sciences, Kanazawa University, 920-8640 Ishikawa, Japan; [b]Laboratory of Animal Physiology, School of Agriculture, Meiji University, 214-8571 Kanagawa, Japan; [c]Department of Anatomy, Faculty of Medicine, Toho University, 143-8540 Tokyo, Japan; [d]Biophotonics Research Group, Exploratory Research Center on Life and Living Systems, National Institutes of Natural Sciences, 444-8787 Okazaki, Japan; and [e]Division of Biophotonics, National Institute for Physiological Sciences, National Institutes of Natural Sciences, 444-8787 Okazaki, Japan

Edited by Erik D. Herzog, Washington University in St. Louis, St. Louis, MO, and accepted by Editorial Board Member Michael Rosbash December 30, 2020 (received for review May 20, 2020)

The suprachiasmatic nucleus (SCN), the central circadian pacemaker in mammals, is a network structure composed of multiple types of γ-aminobutyric acid (GABA)-ergic neurons and glial cells. However, the roles of GABA-mediated signaling in the SCN network remain controversial. Here, we report noticeable impairment of the circadian rhythm in mice with a specific deletion of the vesicular GABA transporter in arginine vasopressin (AVP)-producing neurons. These mice showed disturbed diurnal rhythms of $GABA_A$ receptor-mediated synaptic transmission in SCN neurons and marked lengthening of the activity time in circadian behavioral rhythms due to the extended interval between morning and evening locomotor activities. Synchrony of molecular circadian oscillations among SCN neurons did not significantly change, whereas the phase relationships between SCN molecular clocks and circadian morning/evening locomotor activities were altered significantly, as revealed by PER2::LUC imaging of SCN explants and in vivo recording of intracellular Ca^{2+} in SCN AVP neurons. In contrast, daily neuronal activity in SCN neurons in vivo clearly showed a bimodal pattern that correlated with dissociated morning/evening locomotor activities. Therefore, GABAergic transmission from AVP neurons regulates the timing of SCN neuronal firing to temporally restrict circadian behavior to appropriate time windows in SCN molecular clocks.

circadian rhythm | suprachiasmatic nucleus | GABA | arginine vasopressin

In mammals, the suprachiasmatic nucleus (SCN) of the hypothalamus functions as the central circadian clock, orchestrating multiple circadian biological rhythms in the body (1). The SCN contains ∼20,000 cells, most of which have the ability to generate circadian oscillations. Individual SCN cells have intracellular molecular machinery (molecular clock) driven by autoregulatory transcriptional/translational feedback loops of clock genes in cooperation with cytosolic signaling molecules, such as cAMP and Ca^{2+}. Intriguingly, these molecular clocks are not unique to SCN cells and are common to peripheral cells. Rather, intercellular communications among SCN cells are essential to generate a highly robust, coherent circadian rhythm (1).

The SCN is a cellular network consisting of multiple types of γ-aminobutyric acid (GABA)-ergic neurons, which are categorized according to coexpressed neuropeptides, and astrocytes (1, 2). Arginine vasopressin (AVP)-producing GABAergic neurons represent the SCN shell, the dorsomedial part of the SCN, while vasoactive intestinal polypeptide (VIP)-producing and gastrin-releasing peptide (GRP)-producing GABAergic neurons are located in the SCN core, the ventrolateral part. VIP has been reported to be a critical factor in the maintenance and synchronization of molecular clocks in individual SCN neurons (3, 4). In addition, other neuropeptides, such as AVP and GRP, may also regulate the intercellular communication of SCN neurons (5–7).

In contrast to our advanced knowledge of peptidergic signaling, the functional roles of GABA-mediated signaling in the SCN network remain controversial (8). GABA was initially reported to synchronize action potential firing rhythms of dispersed SCN neurons through $GABA_A$ receptors (9). In contrast, experiments using bioluminescence reporters of clock gene expression (PER2::LUC) in brain slice preparations suggested that $GABA_A$ receptor signaling instead opposes the synchrony of molecular clocks of individual SCN neurons by increasing cycle-to-cycle period variation (10). As for the interaction between the SCN shell and core, GABA signaling resynchronizes the firing rhythms of the two regions after the phase-dissociation caused by phase-shifting light exposure (11). In the SCN from mice housed in an extremely long photoperiod, GABA signaling enhances the resynchronization when PER2::LUC luminescence in the shell and core oscillates in antiphasic configurations, while it opposes the synchrony when these two oscillations are in phase with each other under standard lighting conditions (12).

Significance

In mammals, the suprachiasmatic nucleus (SCN) functions as the master circadian clock to orchestrate multiple circadian biological rhythms in the body. Although almost all SCN neurons contain γ-aminobutyric acid (GABA) as a neurotransmitter, the physiological roles of GABA in the SCN network are poorly understood. We show that mice lacking GABA release specifically from arginine vasopressin (AVP)-producing neurons, one of the major neuron types in the SCN, retain an SCN that progresses normally at the clock gene level but fires aberrantly with bimodal rhythm. Accordingly, the mice demonstrate locomotor activity at inappropriate times with respect to the clock gene-based SCN clock. GABAergic transmission from AVP neurons may regulate SCN firing rhythm to modulate when SCN molecular clocks enable daily behavior.

Author contributions: T.M., Y. Tsuno, and M.M. designed research; T.M., Y. Tsuno, S.M., Y. Tsuneoka, E.H., M.T.I., R.E., T.J.N., and M.M. performed research; T.M., Y. Tsuno, S.M., Y. Tsuneoka, E.H., M.T.I., R.E., T.J.N., and M.M. analyzed data; and T.M., Y. Tsuno, S.M., Y. Tsuneoka, T.J.N., and M.M. wrote the paper.

The authors declare no competing interest.

This article is a PNAS Direct Submission. E.D.H. is a guest editor invited by the Editorial Board.

[1]Present address: International Institute for Integrative Sleep Medicine, University of Tsukuba, 305-8575 Tsukuba, Japan.

[2]To whom correspondence may be addressed. Email: mieda@med.kanazawa-u.ac.jp.

This article contains supporting information online at https://www.pnas.org/lookup/suppl/doi:10.1073/pnas.2010168118/-/DCSupplemental.

Published February 1, 2021.

Thus far, the functional roles of GABA signaling in the central clock have been studied using in vivo and ex vivo pharmacological approaches, which are not suitable to address its neuron type-specific function. Therefore, we hypothesized that neuron type-specific genetic manipulation of GABAergic transmission would be effective in dissecting its role in the generation of circadian rhythm by the SCN network. We previously reported that AVP neurons play a critical role in the generation of circadian rhythm and determination of the circadian period by the SCN network, whose functions may be mediated by transmitters other than AVP peptide (13, 14). Thus, we decided to examine the function of GABA transmission from AVP neurons using a genetic manipulation in which the vesicular GABA transporter gene (*Vgat*, also called *Slc32a1*), which is necessary for filling synaptic vesicles with GABA and thereby for synaptic GABA release (15), is deleted specifically in AVP neurons. Such an

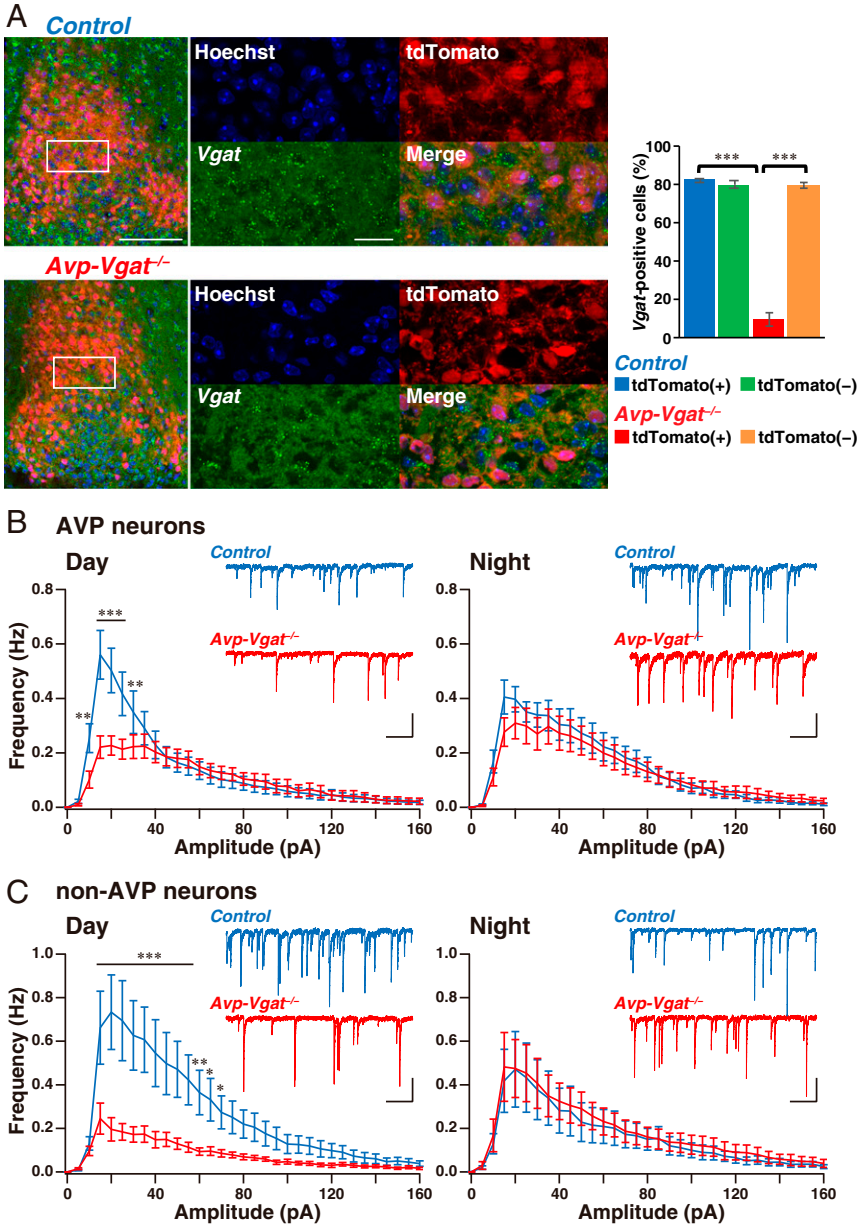

Fig. 1. AVP neuron-specific deletion of *Vgat* reduces the frequency of miniature GABAergic synaptic currents in both AVP neurons and non-AVP neurons during the daytime. (*A*) *Vgat* expression in the SCN of *Avp-Vgat*$^{-/-}$ mice was drastically reduced specifically in AVP neurons. In situ hybridization chain reaction was performed to detect *Vgat* mRNA (green dots) on coronal brain sections prepared from control (*Upper*) and *Avp-Vgat*$^{-/-}$ mice (*Lower*) crossed with *Rosa26-LSL-tdTomato* reporter mice. AVP neurons were identified as tdTomato(+) cells. The locations of the magnified images are indicated by white rectangles in the low-power images. (Scale bars: 100 μm and 20 μm in the left and magnified images, respectively.) (*B*) Amplitude–frequency histograms showing that the mGPSC frequency in AVP neurons from *Avp-Vgat*$^{-/-}$ mice (red line) was significantly reduced in 10- to 30-pA amplitude bins compared to control mice (blue line) during the daytime (*Left*, ZT2 to ZT10, $n = 29$ and 30 from 5 *Avp-Vgat*$^{-/-}$ and 6 control mice, respectively) but not during the nighttime (*Right*, ZT14 to ZT22, $n = 28$ and 26 from 5 *Avp-Vgat*$^{-/-}$ and 5 control mice, respectively). (*C*) The histograms show significant reduction of the mGPSC frequency in non-AVP neurons from *Avp-Vgat*$^{-/-}$ mice across multiple amplitude bins during the daytime specifically (daytime, $n = 18$ and 17 from 4 *Avp-Vgat*$^{-/-}$ and 4 control mice, respectively; nighttime, $n = 21$ and 16 from 4 *Avp-Vgat*$^{-/-}$ and 2 control mice, respectively). (*Inset*) Samples of mGPSCs recorded in control (blue line) and *Avp-Vgat*$^{-/-}$ mice (red line) in each condition. (Scale bars: 0.5 s and 40 pA.) Values are mean ± SEM; $^{*}P < 0.05$, $^{**}P < 0.01$, $^{***}P < 0.001$ by two-way repeated-measures ANOVA followed by post hoc pairwise comparisons.

approach can also avoid the drawback of conventional *Vgat* knockout, which is embryonically lethal (15, 16).

Results

Generation of *Avp-Vgat*$^{-/-}$ Mice That Lack *Vgat* Specifically in AVP Neurons. To generate mice lacking VGAT specifically in AVP neurons, we crossed mice carrying floxed *Vgat* alleles (*Vgat*$^{flox/flox}$) with hemizygous *Avp-Cre* mice that express improved Cre recombinase specifically in AVP neurons (14, 17). These newly generated mice are hereafter referred to as *Avp-Vgat*$^{-/-}$ mice. To quantify the efficiency and specificity of *Vgat* deletion, *Avp-Vgat*$^{-/-}$ mice were further crossed with *Rosa26-LSL-tdTomato* reporter mice (Ai14 mice) (18) to label AVP neurons with red-fluorescent tdTomato. *Vgat* mRNA was detected using in situ hybridization chain reaction (19). In the SCN of *Avp-Vgat*$^{-/-}$*;tdTomato* mice, the number of tdTomato(+);*Vgat*(+) cells was drastically reduced by ∼90% as compared to that of *Avp-Cre;Vgat*$^{wt/flox}$*;tdTomato* ($P < 0.001$), whereas the numbers of tdTomato(−);*Vgat*(+) cells were comparable between genotypes ($P = 0.95$) (Fig. 1*A*). The efficiency was also comparable to the specific deletion of *Bmal1* $^{flox/flox}$ alleles using the same *Avp-Cre* line (14). Thus, *Vgat* was deleted specifically and efficiently from AVP neurons in the SCN of *Avp-Vgat*$^{-/-}$ mice.

GABAergic Synaptic Transmission in Daytime Is Reduced in the SCN of *Avp-Vgat*$^{-/-}$ Mice. We next evaluated the effects of AVP neuron-specific VGAT deletion on GABAergic transmission in the SCN neural network using in vitro electrophysiological experiments. To identify AVP neurons under the microscope using the red fluorescence of tdTomato, we used *Avp-Vgat*$^{-/-}$*;tdTomato* mice with *Avp-Cre;Vgat*$^{wt/flox}$*;tdTomato* mice as controls. In acute coronal brain slices including the SCN, we recorded tetrodotoxin (TTX)-insensitive miniature $GABA_A$ receptor-mediated postsynaptic currents (mGPSCs), a primary measure of synaptic modification, separately from red-fluorescent AVP neurons in the SCN shell and nonfluorescent non-AVP neurons located in the SCN core. Indeed, these mGPSCs completely disappeared in the presence of 10 μM SR95531, a $GABA_A$ receptor antagonist (*SI Appendix*, Fig. S1).

In AVP neurons, we found that the frequency of mGPSCs, especially those of small amplitude (10 to 30 pA), was significantly lower during daytime recordings in *Avp-Vgat*$^{-/-}$ mice compared to that in control mice ($P < 0.001$) (Fig. 1*B*). However, *Avp-Vgat*$^{-/-}$ and control mice showed no difference in mGPSCs during nighttime ($P = 0.67$). Notably, in control mice, the small-amplitude mGPSCs were observed more frequently during daytime rather than nighttime recordings ($P < 0.01$) (*SI Appendix*, Fig. S2*A*), with a tendency to increase during the middle of the day (*SI Appendix*, Fig. S3*A*). In *Avp-Vgat*$^{-/-}$ mice, the daily difference in mGPSC frequency was not clearly observed in AVP neurons ($P = 0.34$). Similarly, in non-AVP neurons of *Avp-Vgat*$^{-/-}$ mice, a reduction in mGPSC frequency was observed across multiple amplitude bins in daytime ($P < 0.001$) but not in nighttime ($P = 0.75$) compared to that in control mice (Fig. 1*C*). The frequency of mGPSCs in non-AVP neurons of control mice was higher in the middle of the day (*SI Appendix*, Fig. S3*B*), although the daily difference was not clearly seen in the amplitude-frequency histogram (*SI Appendix*, Fig. S2*B*) ($P = 0.24$). In contrast, mGPSCs were detected more frequently during nighttime than during daytime in non-AVP neurons of *Avp-Vgat*$^{-/-}$ mice ($P < 0.001$) (*SI Appendix*, Figs. S2*B* and S3*B*).

Because SCN neurons have been shown to receive inputs from AVP neurons, as well as from neurons in the SCN core (20), the significant reduction in mGPSC frequency in the SCN neurons of *Avp-Vgat*$^{-/-}$ mice suggested that the AVP neuron-specific deletion of *Vgat* successfully depressed the synaptic release of GABA from AVP neurons in the SCN network. These data also suggest that the mGPSC components that are dominantly detected in the daytime in control mice and disappear in *Avp-Vgat*$^{-/-}$ mice may be caused by GABA released from AVP neuron terminals. Furthermore, the mGPSCs remaining in *Avp-Vgat*$^{-/-}$ mice are likely postsynaptic events induced by GABA released from non-AVP neuronal terminals, which were more frequent at night. Thus, the efficacy of GABAergic transmission from AVP neuron terminals

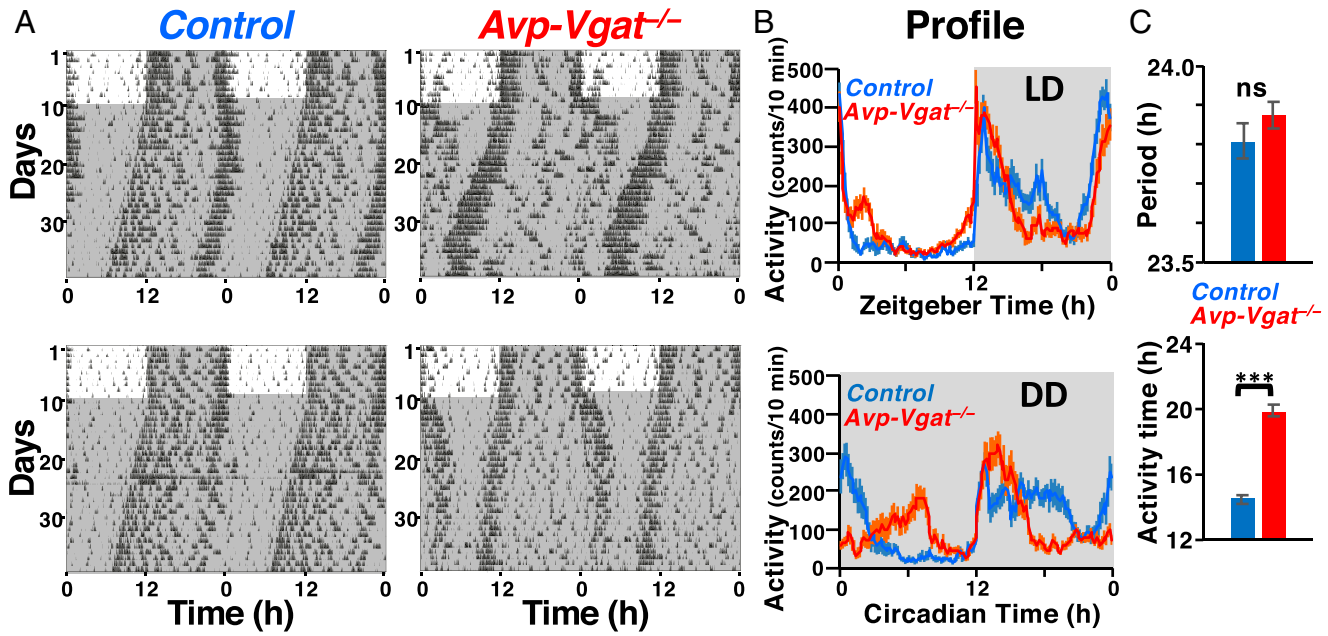

Fig. 2. *Avp-Vgat*$^{-/-}$ mice show lengthening of the activity time. (*A*) Representative locomotor activity of two control and two *Avp-Vgat*$^{-/-}$ mice. Animals were initially housed in 12:12-h LD conditions and then transferred to DD. Gray shading indicates the time when lights were off. (*B*) Averaged daily profile of locomotor activity in LD or DD. (*C*) The mean free-running period and the activity time in DD. Values are mean ± SEM; $n = 13$ for control, $n = 15$ for *Avp-Vgat*$^{-/-}$ mice. ***$P < 0.001$ by two-tailed Student's *t* tests; ns, not significant.

and non-AVP neuron terminals shows a diurnal variation in a pathway-specific manner (*SI Appendix*, Fig. S2*C*).

***Vgat* Deficiency in AVP Neurons Lengthened the Activity Time in the Circadian Behavioral Rhythm.** To examine the fundamental roles of GABAergic transmission from SCN AVP neurons in the generation of circadian rhythms, we next measured the spontaneous locomotor activity in *Avp-Vgat*$^{-/-}$ mice. The behavior of these mice was significantly different from that of control mice (*Vgat*$^{flox/flox}$ and *Avp-Cre;Vgat*$^{wt/flox}$ mice; these two behaved similarly) in 12 h of light and 12 h of darkness (LD12:12) (Fig. 2 and *SI Appendix*, Tables S1 and S2). Nocturnal activities in both groups were bimodal, showing morning and evening components of locomotor activity. The daily activity profile showed that the activity onset was significantly earlier and the activity offset was later, and thus the activity time was longer, in *Avp-Vgat*$^{-/-}$ mice compared to that in control mice (activity onset, zeitgeber time [ZT]11.21 ± 0.18 vs. ZT12.04 ± 0.04, $P < 0.001$; activity offset, ZT2.90 ± 0.36 vs. ZT1.16 ± 0.26, $P < 0.001$; activity time, 15.69 ± 0.36 h vs. 13.12 ± 0.27 h, $P < 0.001$) (Fig. 2 *A* and *B* and *SI Appendix*, Table S1). Although the activity time was lengthened, the activity count did not differ significantly, resulting in a more profound drop in activity level in the middle of the dark phase.

In constant darkness (DD), *Avp-Vgat*$^{-/-}$ mice showed an activity pattern drastically different from that of control mice (Fig. 2 and *SI Appendix*, Table S1). When released into DD, the activity time gradually lengthened. After ∼1 wk in DD, the activity time reached a steady-state length ∼5.5 h longer than that in controls (19.92 ± 0.27 h vs. 14.47 ± 0.27 h, $P < 0.001$; days 15 to 22 in DD), increasing the phase difference between morning and evening locomotor activity components. The circadian amplitude (periodogram Qp value), free-running period, total daily activity, and activity during the activity time were not significantly different between the two groups (Fig. 2 and *SI Appendix*, Table S1). These results indicate that the SCN output is conveyed to the brain regions regulating locomotor activity, but the timing of the output to behavior is incorrect in *Avp-Vgat*$^{-/-}$ mice.

Importantly, the lengthening of the activity time in *Avp-Vgat*$^{-/-}$ mice was reversed almost completely when *Vgat* expression was restored in the AVP neurons of the SCN using a recombinant adeno-associated virus (AAV) vector (*SI Appendix*, Fig. S4 and Table S3). This result suggests that the lack of GABA release from SCN AVP neurons, but not from AVP neurons outside the SCN nor the developmental defects of neuronal connectivity of the SCN network, account for the impaired circadian behavior in *Avp-Vgat*$^{-/-}$ mice.

***Vgat* Is Not Necessary to Transmit the Cellular Period of AVP Neurons.** The lengthened activity time observed in *Avp-Vgat*$^{-/-}$ mice was a feature shared with *Avp-Bmal1*$^{-/-}$ mice, in which the disruption of molecular clocks in SCN AVP neurons results in the lengthening of both activity time and free-running period (14). In addition, AVP neurons function as at least a part of the pacemaker cells of the SCN that transmit the period of their own molecular clocks to the behavioral period (13). Taking these observations into account, we next examined whether the transmission of the cellular period from AVP neurons depends on GABAergic signaling. When the cellular period of AVP neurons was artificially lengthened by deleting the casein kinase 1δ (*CK1δ*) gene specifically in these cells (*Avp-CK1δ*$^{-/-}$ mice: here *Avp-Cre;Vgat*$^{wt/flox}$;*CK1δ*$^{flox/flox}$ mice), the free-running period of the behavioral rhythm was also lengthened while the activity time was not changed, as we previously reported (free-running period, 24.93 ± 0.10 h vs. 23.79 ± 0.07 h, $P < 0.001$; activity time, 13.85 ± 0.61 h vs. 14.20 ± 0.89 h, $P > 0.05$) (*SI Appendix*, Fig. S5 and Table S4) (13). Notably, mice in which AVP neurons lacked both *Vgat* and *CK1δ* (*Avp-Vgat*$^{-/-}$;*CK1δ*$^{-/-}$ mice) exhibited a circadian behavior that seemed to have both properties of *Avp-Vgat*$^{-/-}$ mice and *Avp-CK1δ*$^{-/-}$ mice and resembled those of *Avp-Bmal1*$^{-/-}$ mice (free-running period, 24.74 ± 0.06 h; activity time, 20.27 ± 0.45 h) (*SI Appendix*, Fig. S5 and Table S4) (14). Since *Avp-Vgat*$^{-/-}$;*CK1δ*$^{-/-}$ mice were still capable of reflecting the lengthening of the cellular period in the free-running behavior period, the transmission of the period length of AVP neurons' molecular clocks to the entire SCN network and other brain regions regulating locomotor activity may not depend on GABA-mediated signaling from AVP neurons.

Circadian Gene Expression In Vivo Is Normal in the SCN of *Avp-Vgat*$^{-/-}$ Mice. We next evaluated the in vivo state of molecular clocks in the SCN of *Avp-Vgat*$^{-/-}$ mice by measuring *Avp* and *Per1* mRNA levels using in situ hybridization (Fig. 3). In the SCN of control mice, as expected, *Avp* mRNA was expressed predominantly in the shell and showed a clear circadian pattern in expression on the first day in DD (21). Similarly, a core component of the

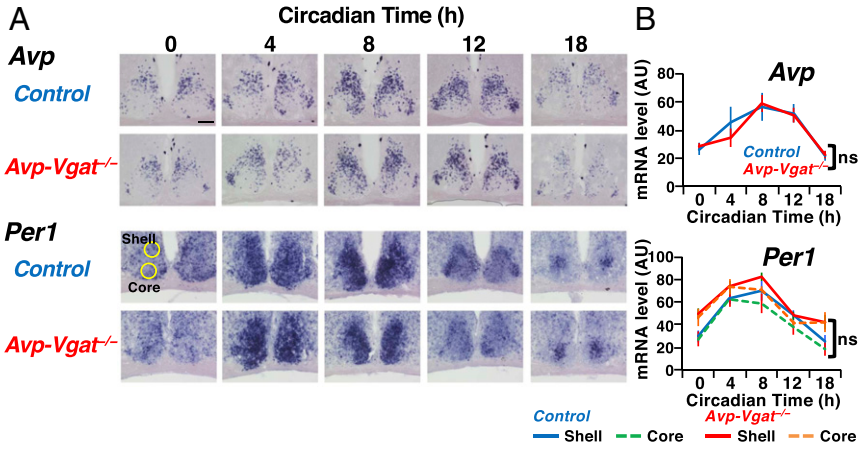

Fig. 3. Circadian gene expression is not altered in the SCN of *Avp-Vgat*$^{-/-}$ mice. (*A*) Representative images of *Avp* and *Per1* mRNA expression in the SCN of control and *Avp-Vgat*$^{-/-}$ mice at the time indicated. Coronal brain sections were hybridized in situ to an antisense probe for each gene. (Scale bar, 100 μm.) (*B*) Circadian expression of each gene in the middle SCN along the rostrocaudal axis. Expression was quantified for the entire SCN (*Avp*) or separately for the shell and core (*Per1*) and expressed in arbitrary units (AU). Statistically significant difference was not detected in the expression of either gene. Representative regions defined as the shell and core SCN are indicated by yellow circles in *A*. Values are mean ± SEM; $n = 6$. No statistically significant effects of genotype were detected by two-way repeated-measures ANOVA followed by post hoc pairwise comparisons (ns).

molecular clocks, *Per1*, was expressed in a circadian manner both in the SCN shell and the core (22, 23). Despite their impaired behavioral rhythm, circadian expression of these genes in the SCN of *Avp-Vgat*$^{-/-}$ mice did not differ significantly from that in control mice. These data suggest that clock gene-based molecular clocks in the SCN oscillated normally in vivo.

Behavioral Output Is Temporally Misaligned to the SCN Molecular Clocks in *Avp-Vgat*$^{-/-}$ Mice. The increase in phase difference between morning and evening locomotor activity components in the circadian behavioral rhythm of *Avp-Vgat*$^{-/-}$ mice may implicate attenuated synchronization of SCN neurons (14, 24, 25). To test this hypothesis, we performed real-time bioluminescent cell imaging of coronal SCN slices prepared from control and *Avp-Vgat*$^{-/-}$ mice with a luciferase reporter (*Per2::Luc*) (26) (*Avp-Vgat*$^{-/-}$*;Per2::Luc* mice) housed in DD for at least 2 wk (Fig. 4). We expected that the amplitude of the PER2::LUC bioluminescent oscillation might be reduced in the mutant mice, which might suggest an attenuated synchrony of SCN molecular clocks. However, the amplitude as well as the period of PER2::LUC oscillation were comparable between the two groups, both in the SCN shell and core (Fig. 4*B*). Importantly, the peak phase of PER2::LUC oscillations in *Avp-Vgat*$^{-/-}$*;Per2::Luc* mice was delayed by 1.9 h relative to that in *Control;Per2::Luc* mice (Fig. 4 *A* and *C*). The peak phase was around projected circadian time (CT)12.5 in both the SCN shell and core of control mice, as reported previously (shell, CT12.33 ± 0.25; core, CT12.70 ± 0.25) (26), while it was around projected CT14.5 in *Avp-Vgat*$^{-/-}$*;Per2::Luc* mice (shell, CT14.23 ± 0.14; core, CT14.51 ± 0.22). Because CT12 was defined as the time of locomotor activity onset, these results suggested that the activity onset was advanced relative to the SCN molecular clocks as defined by PER2::LUC oscillations in *Avp-Vgat*$^{-/-}$*;Per2::Luc* mice in comparison to that in control mice. In contrast, the activity offset was significantly delayed relative to the SCN clock, by ∼4 h, in mutant mice as compared to that in controls (time lag between activity offset and PER2::LUC peak in the SCN shell, 5.28 ± 0.32 h vs. 1.04 ± 0.47 h, $P < 0.001$; that in the SCN core, 5.00 ± 0.49 h vs. 0.67 ± 0.53 h, $P < 0.001$), which was consistent with the lengthening of the activity time by ∼5.5 h in *Avp-Vgat*$^{-/-}$ mice (Fig. 2).

To increase the spatial resolution of circadian rhythm analysis, we applied a cosine curve-fitting method to PER2::LUC oscillations in individual pixels that covered the SCN (Fig. 4 *D–G*) (27). As observed in the region-of-interest analyses described above, the mean period and amplitude of individual pixel oscillations were comparable between *Control;Per2::Luc* and *Avp-Vgat*$^{-/-}$*;Per2::Luc* mice. Notably, the SD of the first peak phase, whose increase is an indicator of reduced synchrony between pixels' PER2::LUC oscillations, did not change significantly in *Avp-Vgat*$^{-/-}$*;Per2::Luc* mice in comparison with the controls both in the shell and core. In contrast, the delayed peak phases in *Avp-Vgat*$^{-/-}$*;Per2::Luc* mice observed in region-of-interest analysis (Fig. 4*C*) were reproduced by the pixels' PER2::LUC oscillations (mean peak phase in the shell, CT13.97 ± 0.30 vs. CT11.84 ± 0.35, $P < 0.001$; core, CT14.18 ± 0.21 vs. CT12.61 ± 0.27, $P < 0.01$) (Fig. 4 *F* and *G*). The spatiotemporal order of PER2::LUC oscillations in four regions within the SCN (28) were comparable between *Control;Per2::Luc* and *Avp-Vgat*$^{-/-}$*;Per2::Luc* mice, although the peak phases were delayed evenly in the latter (*SI Appendix*, Fig. S6). Collectively, these data obtained from PER2::LUC imaging suggested that the spatiotemporal organization of molecular clocks may be almost intact in the SCN explants of *Avp-Vgat*$^{-/-}$*;Per2::Luc* mice. Rather, the lack of GABAergic transmission from AVP neurons may impair the timing of SCN outputs to behavior without altering the molecular clocks of the SCN.

Temporal Relationship between the Locomotor Activity and In Vivo Ca^{2+} Rhythm of SCN AVP Neurons Is Disturbed in *Avp-Vgat*$^{-/-}$ Mice. We next examined the in vivo temporal relationship between the circadian behavioral rhythm and SCN molecular clocks by simultaneously recording the spontaneous locomotor activity and the intracellular Ca^{2+} ($[Ca^{2+}]_i$) rhythm in SCN AVP neurons using fiber photometry in *Avp-Vgat*$^{-/-}$ and control mice (*Avp-Cre* and *Avp-Cre;Vgat*$^{wt/flox}$ mice) (Fig. 5 and *SI Appendix*, Figs. S7 and S8) (29). $[Ca^{2+}]_i$ rhythms in the SCN have been shown to be an excellent measure of molecular clocks containing both TTX-sensitive and -insensitive mechanisms that can be recorded in vivo in a neuron type-specific manner using genetically encoded calcium sensors and fiber photometry (27, 30–32). To do this, we specifically expressed the fluorescent Ca^{2+} indicator jGCaMP7s (33) in the neurons by focally injecting a Cre-dependent AAV vector (*SI Appendix*, Fig. S8*C*). Importantly, our fiber photometry method did not detect significant circadian oscillation of fluorescence when control EGFP was expressed in the SCN AVP neurons (*SI Appendix*, Figs. S7*B* and S8*A*). In addition, the $[Ca^{2+}]_i$ rhythm in SCN VIP neurons demonstrated a pattern different from that of SCN AVP neurons described below and perfectly recapitulated a similar recording by Mei et al. (31) when jGCaMP7s was expressed in VIP neurons of *Vip-ires-Cre* mice (34) (*SI Appendix*, Fig. S8*B*). Thus, our measurements of jGCaMP7s fluorescence described below are likely to reflect $[Ca^{2+}]_i$ in AVP neurons correctly.

In LD, a daily $[Ca^{2+}]_i$ rhythm was observed in SCN AVP neurons of control mice, with its peak around the onset of the light phase (ZT23.75 ± 0.26) (Fig. 5 *A* and *B* and *SI Appendix*, Fig. S8*D*). *Avp-Vgat*$^{-/-}$ mice also demonstrated daily $[Ca^{2+}]_i$ rhythms in these neurons. However, its peak occurred significantly later (ZT2.04 ± 0.46, $P < 0.01$, $n = 4$) (Fig. 5 *A* and *B* and *SI Appendix*, Fig. S8*D*) than that in control mice. Such $[Ca^{2+}]_i$ rhythms continued in DD in both groups. When released into DD, as shown earlier (Fig. 2), the circadian behavioral rhythm in *Avp-Vgat*$^{-/-}$ mice demonstrated a gradual increase in activity time due to the increased phase difference between evening and morning locomotor activity components (Fig. 5*B* and *SI Appendix*, Fig. S8*E*). Free-running periods during DD8 to DD10 were comparable between behavior and $[Ca^{2+}]_i$ rhythms, as well as between control and *Avp-Vgat*$^{-/-}$ mice (*SI Appendix*, Fig. S8 *F–H*). Notably, the temporal relationship between the peak phase of $[Ca^{2+}]_i$ rhythm and locomotor activity offset was altered in *Avp-Vgat*$^{-/-}$ mice (Fig. 5). The activity offset slightly preceded the peak of the $[Ca^{2+}]_i$ rhythm in control mice, while it was gradually delayed beyond the $[Ca^{2+}]_i$ peak in *Avp-Vgat*$^{-/-}$ mice (ΔPhase [offset], −1.51 ± 0.83 h vs. 3.80 ± 1.33 h in DD8 to DD10, $P < 0.05$) (Fig. 5 *C*, *Right*). The phase relationship between the activity onset and $[Ca^{2+}]_i$ peak did not differ significantly between the two groups (ΔPhase [onset], 10.00 ± 0.69 h vs. 9.37 ± 1.13 h in DD8 to DD10, $P = 0.65$) (Fig. 5 *C*, *Left*). The observed temporal misalignment of locomotor activity and $[Ca^{2+}]_i$ rhythms in vivo was in agreement with the results of PER2::LUC rhythms in SCN slices, supporting the idea that GABAergic transmission from AVP neurons may regulate correctly timed outputs from SCN molecular clocks to behavior.

In Vivo Neuronal Activity of the SCN Exhibits Bimodal Rhythm in *Avp-Vgat*$^{-/-}$ Mice. Neuronal firing of SCN neurons is a principal output signal conveyed to the extra-SCN areas. Upon the apparent normal spatiotemporal organization of molecular clocks in the SCN of *Avp-Vgat*$^{-/-}$ mice, we examined the neuronal activity rhythms of the SCN in freely moving mice by recording multiunit activity (MUA) in vivo with simultaneous monitoring of wheel-running locomotor activity. As reported previously, control mice exhibited clear unimodal daily rhythms of SCN MUA in both LD and DD, which were approximately antiphasic to locomotor activity (Fig. 6 *A* and *B* and *SI Appendix*, Fig. S9) (35–37).

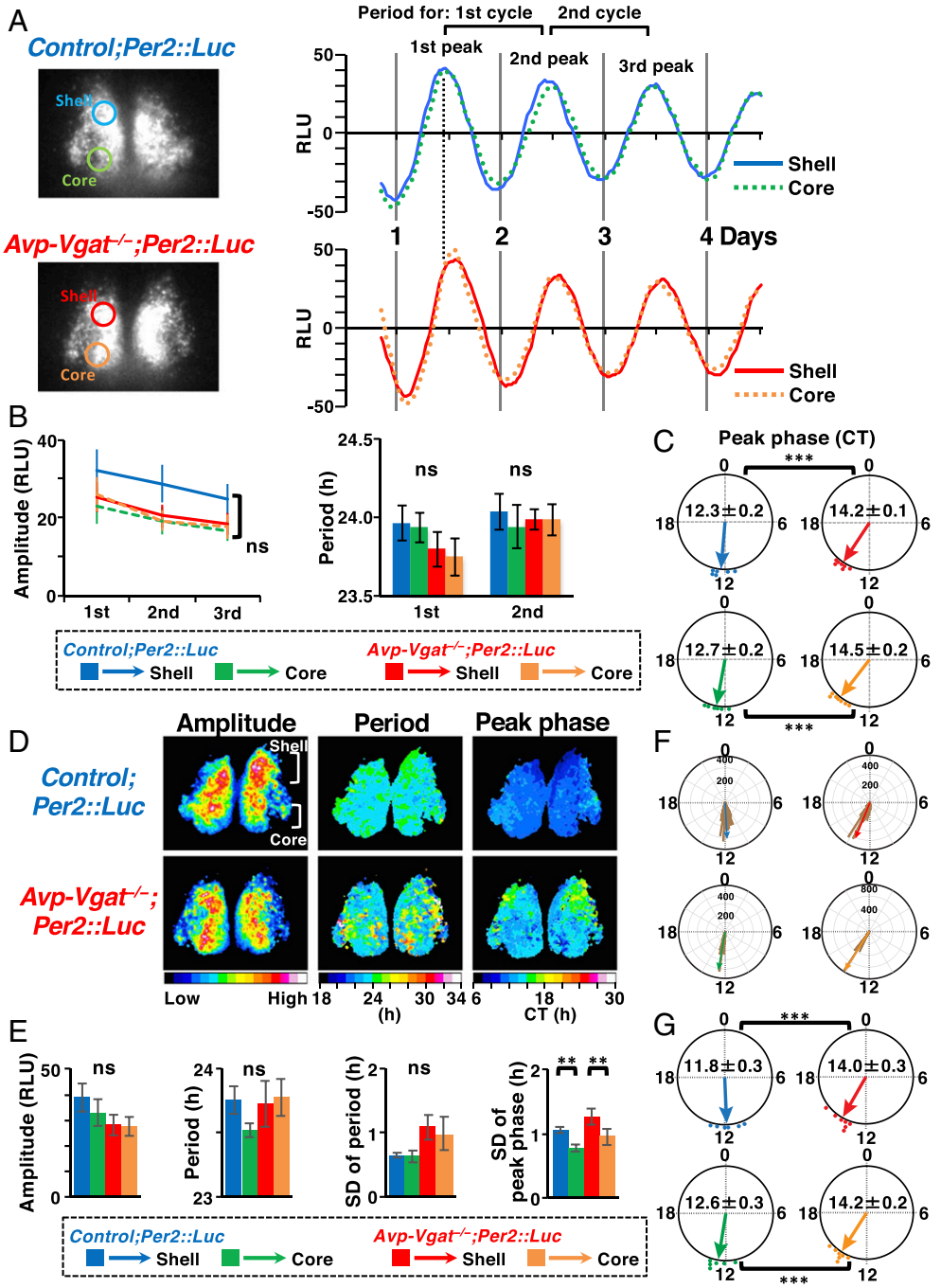

Fig. 4. Phase relationships between SCN molecular clocks and the locomotor activity rhythm are altered in *Avp-Vgat*$^{-/-}$ mice. (*A*) Representative images of PER2::LUC expression. Coronal SCN slices of the midrostrocaudal region were prepared from adult control and *Avp-Vgat*$^{-/-}$ mice with a luciferase reporter (*Per2::Luc*) housed in DD. Detrended bioluminescence expressed in relative light units (RLU) within the shell and core regions indicated in the images were plotted on the right. Gray vertical lines labeled "Day 1" indicate around CT0 (16 h after the start of image recordings around CT8). (*B*) Amplitude of the three peaks defined in *A* and periods of PER2::LUC oscillations for two cycles. (*C*) The first peak phases in CT according to behavioral free-running period before slice preparation were shown as Rayleigh plots. Dots indicate the first peak phases of each slice and arrows indicate mean resultant vectors of them. The peak phase was significantly delayed in the SCN *Avp-Vgat*$^{-/-}$*;Per2::Luc* mice. (*D*) Representative amplitude, period, and first peak phase maps of PER2::LUC oscillation at the pixel level of SCN slices shown in *A*. Amplitude, period, and peak phase of PER2::LUC oscillations in the individual pixels covering the SCN were calculated by cosine curve fittings for data representing 72 h from the first CT6 after slice preparation. The dorsal 40% and ventral 30% regions of the SCN were regarded as the shell and core, respectively. Representative regions defined as the SCN shell or core are indicated. (*E*) Mean amplitude, mean period, SD of period, and SD of first peak phase of individual pixels' PER2::LUC oscillations obtained for each region of individual slices are collected and compared between groups. (*F*) Rose plots of pixel's first peak phases for each region in representative slices. The circular histograms in light brown and numbers in each circle indicate the distribution of individual pixels' peak phases. Arrows indicate the mean resultant vectors. (*G*) Rayleigh plots of mean first peak phases of individual pixels' PER2::LUC oscillations. Mean first peak phases of individual pixels' PER2::LUC oscillations were delayed in both SCN shell and core of *Avp-Vgat*$^{-/-}$*;Per2::Luc* mice. Values are mean ± SEM; $n = 6$ for control, $n = 7$ for *Avp-Vgat*$^{-/-}$*;Per2::Luc* mice. $^{**}P < 0.01$; $^{***}P < 0.001$ by two-way repeated-measures ANOVA followed by post hoc pairwise comparisons (*B* and *E*), or by Harrison–Kanji test followed by Watson–Williams test (*C* and *G*). *P* values of Rayleigh test were <0.001 for all circular data.

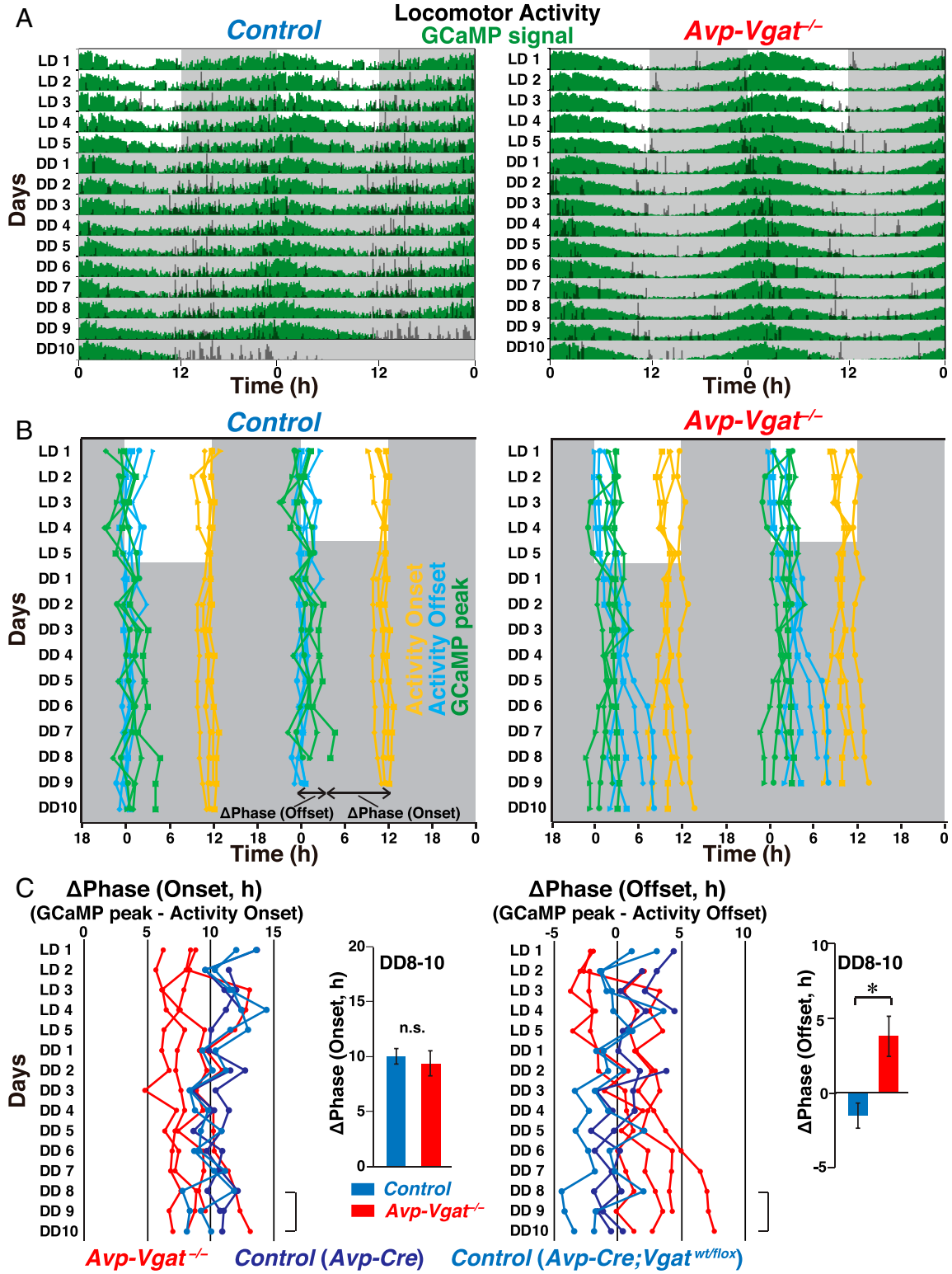

Fig. 5. Temporal relationship between the in vivo intracellular Ca^{2+} rhythm of SCN AVP neurons and locomotor activity is disturbed in *Avp-Vgat*$^{-/-}$ mice. (*A*) Representative plots of the in vivo jGCaMP7*s* signal of SCN AVP neurons (green) overlaid with locomotor activity (black) in actograms. Control (*Left*) and *Avp-Vgat*$^{-/-}$ (*Right*) mice were initially housed in LD (LD1 to LD5) and then in DD (DD1 to DD10). The dark periods are represented as gray shaded areas. (*B*) Plots of locomotor activity onset (orange), activity offset (light blue), and the peak phase of the GCaMP signal (green) in individual control (*Left*) and *Avp-Vgat*$^{-/-}$ (*Right*) mice. Identical marker shapes indicate data from the same animal. (*C*) Plots of the phase difference between activity onset and GCaMP peak (*Left*) or activity offset and GCaMP peak (*Right*). Positive values in ΔPhase (GCaMP peak – activity onset/offset) indicate that the GCaMP peak is earlier than the activity onset/offset. Red, *Avp-Vgat*$^{-/-}$; dark blue, control (*Avp-Cre*); light blue, control (*Avp-Cre;Vgat*$^{wt/flox}$). The average of values during DD8 to DD10 was compared between groups in bar graphs; mean ± SEM; $n = 4$. *$P < 0.05$ by two-tailed Student's *t* test.

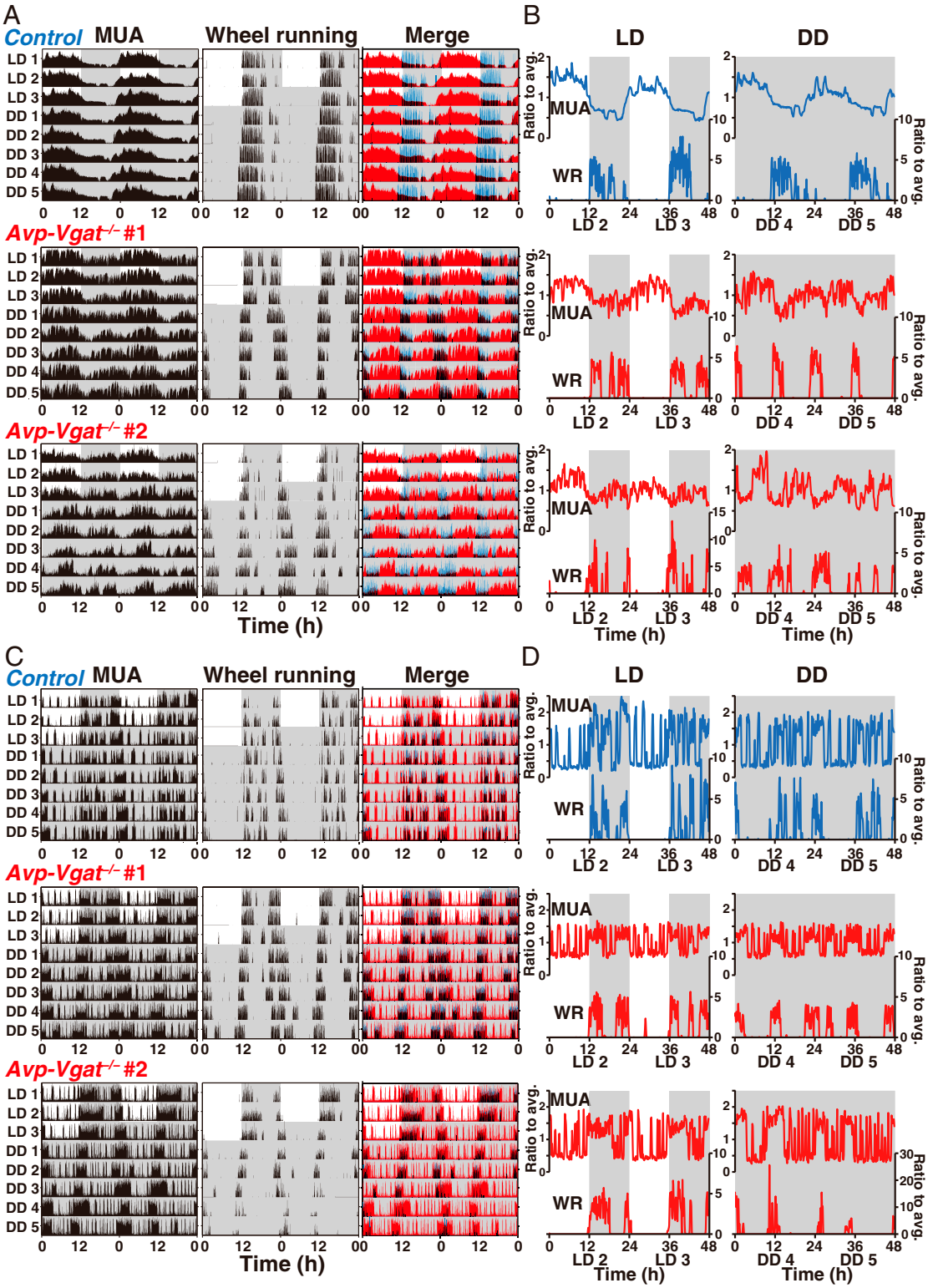

Fig. 6. In vivo MUA of the SCN exhibits daily bimodal rhythm in *Avp-Vgat*$^{-/-}$ mice. (*A*) Representative actograms of in vivo MUA rhythm in the SCN of a control and two *Avp-Vgat*$^{-/-}$ mice. Animals were initially housed in LD (LD1 to LD3) and then in DD (DD1 to DD5). The dark periods are represented as gray shaded areas. The MUA (*Left*), wheel running (WR) activity (*Center*), and overlaid (*Right*; red: MUA, blue: WR) are shown. (*B*) Serial plots of MUA in the SCN (*Upper*) and WR (*Lower*) in the last 48 h of LD or DD. Ten-minute average counts were normalized with 48 h average. (*C*) Representative actograms of in vivo MUA rhythm outside SCN of a control and two *Avp-Vgat*$^{-/-}$ mice. (*D*) Serial plots of MUA outside SCN (*Upper*) and WR (*Lower*) in the last 48 h of LD or DD.

In *Avp-Vgat*$^{-/-}$ mice, by clear contrast, SCN MUA still exhibited a daily rhythm but a higher level during the night in LD or subjective night in DD, shaping an additional wave (Fig. 6 *A* and *B* and *SI Appendix*, Fig. S9). Such a bimodal pattern of MUA rhythm was more obvious in DD. Intriguingly, the widths and shapes of waves in the subjective day and night gradually changed

after being released into DD. The morning and evening locomotor activity mostly occurred at drops in the MUA, showing gradual expansion of the activity time in DD, as described previously (Fig. 2). Notably, MUA rhythms in the areas outside the SCN were largely synchronized with locomotor activity in both control and *Avp-Vgat*$^{-/-}$ mice (Fig. 6 *C* and *D*), which was consistent with previous findings in wild-type rodents (35, 37). These data suggest that the lack of GABAergic transmission from AVP neurons causes a bimodal daily rhythm of the SCN MUA, which may increase the phase difference of morning/evening locomotor activity components.

Discussion

In this study, *Vgat* deletion specific to AVP neurons was shown to cause a significant reduction in mGPSC frequency and disrupt its daily variation in the SCN. The mice with this genetic manipulation showed a lengthened activity time but no change in the free-running period of the circadian behavioral rhythm. Cellular PER2::LUC oscillations in the SCN slices were normal, except that the phase relationships between the behavioral rhythm and PER2::LUC rhythm in the SCN were drastically altered in *Avp-Vgat*$^{-/-}$ mice. The onset of locomotor activity was advanced and the end of activity was delayed relative to the SCN molecular clock. Similar temporal misalignment was also observed in vivo between the $[Ca^{2+}]_i$ rhythm of SCN AVP neurons and behavioral rhythm. In *Avp-Vgat*$^{-/-}$ mice, the in vivo firing rhythm of SCN neurons showed a bimodality, which correlated with the dissociated morning/evening locomotor activities. These data suggest that GABAergic transmission from AVP neurons shapes the SCN neuronal activity rhythm to coordinate the time at which the SCN molecular clocks allow the animal's daily behavior.

Daily Rhythms of GABAergic Transmissions in the SCN. In *Avp-Vgat*$^{-/-}$ mice, the frequency of mGPSCs recorded in AVP neurons and non-AVP neurons in the SCN was shown to be highly reduced in daytime but not in nighttime in comparison to that in control mice. Since the frequency of action potential-independent miniature (m) postsynaptic events is generally considered as the parameter to monitor changes in presynaptic transmitter releasing machinery, these data strongly suggest that genetic deletion of VGAT specific to AVP neurons successfully hampered GABA release from AVP neurons in the SCN. AVP neurons, as well as core neurons, reportedly receive projections from both AVP neurons and non-AVP neurons (20). Interestingly, AVP projections have been reported to make extremely sparse contact with VIP neurons. Therefore, the non-AVP neurons in which mGPSCs were detected in this study might be GRP, calretinin-containing, or other neurons, except VIP neurons.

Previously, Itri et al. (38, 39) reported the daily rhythms of the frequency of GABAergic spontaneous inhibitory postsynaptic currents (sIPSCs) in the dorsal SCN neurons that peaked between ZT11 and ZT15 but not in the ventromedial SCN neurons. Furthermore, the frequency of mIPSCs (recorded in the presence of TTX) did not change significantly, although it tended to be higher during the day than during the night (39). In this study, we recorded mGPSCs in a neuron type-specific manner and further calculated the frequency distribution of their amplitude, which successfully revealed their significant day/night differences. The daily rhythms of sIPSCs are affected by the daily fluctuation of presynaptic neuronal firing.

Generation of TTX-insensitive mGPSCs is generally considered to be independent of presynaptic neuronal firing and directly reflects the probability of GABA release regulated at the release sites. Therefore, the daily variation in mGPSC frequency suggests that GABA release from SCN neurons may be under the control of molecular clocks via circadian expression of proteins involved in vesicle exocytosis machinery and presynaptic receptor-mediated modulation of transmitter release, such as an astrocytic glutamatergic signaling affecting presynaptic $[Ca^{2+}]_i$ (2, 40). Indeed, mice lacking *Bmal1* specifically in AVP neurons also exhibit the expansion of activity time as *Avp-Vgat*$^{-/-}$ mice do (14).

Both the inhibitory and excitatory effects of GABA on SCN neurons have been reported, which may differ according to the time of the day, photoperiod, or region within the SCN (8, 11, 41, 42). Whether inter-AVP neuronal and AVP neuron→non-AVP neuron GABAergic transmissions are inhibitory or excitatory would be intriguing to elucidate. In addition to phasic activation of $GABA_A$ receptors through direct synaptic transmission, tonic activation of extrasynaptic $GABA_A$ receptors and $GABA_B$ receptors in SCN neurons should be taken into account as functional elements embedded in the central clock (8).

Increased Phase Difference of Morning and Evening Behavioral Rhythms in *Avp-Vgat*$^{-/-}$ Mice. We first considered the possibility that the disturbed circadian behavioral rhythm of *Avp-Vgat*$^{-/-}$ mice is simply due to the attenuation of GABAergic output from the SCN to the extra-SCN regions that regulate locomotor activity, rather than the impairment of the SCN central circadian clock per se. Attenuation of SCN output should simply affect the amount of activity but not alter the temporal pattern of locomotor activity. However, the result was the opposite; the temporal pattern, but not the amount, of locomotor activity was drastically changed in *Avp-Vgat*$^{-/-}$ mice. In addition, we clearly observed gradual expansion of the activity time in these mice after changing the lighting condition from LD to DD, as if coupling of multiple SCN oscillators (e.g., morning and evening oscillators) transitioned gradually from a stable state in LD to that in DD (24, 43). Furthermore, in *Avp-Vgat*$^{-/-}$*;CK1δ*$^{-/-}$ mice, the lengthened cellular period caused by *CK1δ* deletion in AVP neurons was successfully transmitted to the behavioral rhythm merged with the lengthened activity time of *Avp-Vgat*$^{-/-}$ mice. Collectively, it seems rational to conclude that impairment of the SCN central clock itself accounts for the phenotype of *Avp-Vgat*$^{-/-}$ mice.

Therefore, it was surprising for us that the spatiotemporal organization of molecular clocks was almost normal in the SCN of *Avp-Vgat*$^{-/-}$ mice despite the increased phase difference of morning/evening behavioral rhythms, suggesting the attenuation of coupling among SCN clock neurons. Importantly, in *Avp-Vgat*$^{-/-}$ mice, phase relationships between the SCN time measured based on PER2::LUC molecular clocks and the onset and offset of locomotor activity were considerably altered. It is possible that GABA from AVP neurons simply phase-shifted the molecular clocks in the SCN. However, it seems difficult to explain the phenotype based on such a simple mechanism by itself because the onset and offset of locomotor activity were shifted in the opposite direction with respect to the PER2::LUC clocks. An alteration in the phase relationship was also observed in vivo between the offset of locomotor activity and $[Ca^{2+}]_i$ rhythm in SCN AVP neurons. Taking these data together, we find that GABAergic transmission from AVP neurons may appropriately set the timing of morning and evening components of behavior without significantly influencing oscillations of molecular clocks. The peak phase of the $[Ca^{2+}]_i$ rhythm in SCN AVP neurons at dawn in control mice perfectly matched the daily rhythm of cerebrospinal fluid AVP level in vivo (44). Furthermore, it occurs earlier than that in SCN VIP neurons, which has been seen in the middle of the day using fiber photometry recordings by us (*SI Appendix*, Fig. S8*B*) and others (31, 32). This 5- to 6-h difference in peak phases in vivo between AVP neurons and VIP neurons was consistent with an observation in neonatal SCN cultures (45).

Although the SCN molecular clocks appeared to progress almost normally, SCN neuronal activities exhibited an aberrant, bimodal daily rhythm in *Avp-Vgat*$^{-/-}$ mice. Therefore, the absence

of GABA release from AVP neurons might alter the temporal and spatial patterns of GABA-mediated modulation within the SCN and consequently influence the daily firing rhythms of SCN output neurons that regulate locomotor activity, especially in DD. The fact that abnormalities of behavior, $[Ca^{2+}]_i$, and MUA rhythms were milder in LD, may indicate that light-induced GABA release from non-AVP neurons in the SCN partially compensated for the loss of GABA from AVP neurons. These output neurons may overlap AVP neurons, non-AVP neurons, or both. Further studies are required to identify such output neurons as well as to understand how GABAergic transmission of AVP neurons shapes SCN firing rhythms.

Ono et al. (16) found that the cultured fetal SCN of systemic *Vgat*$^{-/-}$ mice retained normal circadian PER2::LUC rhythms, but showed a unimodal firing rhythm with frequent burst firing throughout 24 h. Furthermore, by focally injecting a ubiquitously Cre-expressing AAV vector into the SCN of adult *Vgat*$^{flox/flox}$ mice to avoid embryonic lethality in *Vgat*$^{-/-}$ mice, they demonstrated that partial *Vgat* deletion in the SCN and its surrounding areas reduces the amplitude of circadian behavioral rhythm but does not lengthen the activity time. Nonspecific but less complete deletion of *Vgat* might reduce GABA release from SCN neuronal terminals in the extra-SCN areas regulating locomotor activity and mask the importance of GABA within the SCN. Importantly, we failed to observe any signs of burst firing in the SCN MUA of *Avp-Vgat*$^{-/-}$ mice. Indeed, application of the $GABA_A$ antagonist bicuculline to the SCN slices of adult rats has not been reported to cause burst firing (11). Thus, Ono et al. (16) and our present study showed that VGAT is not critical for SCN PER2::LUC rhythms but demonstrate different circadian phenotypes of different genetic manipulations and ages. Intriguingly, a recent study reported that selective deletion of *Vgat* in VIP neurons produced no discernable disruption in circadian rhythms of locomotor activity and body temperature, suggesting a specialized role of GABA released from AVP neurons in the SCN network (46).

Conclusions

The present study addresses the function of GABAergic transmissions in the central circadian pacemaker of the SCN by means of neuron type-specific genetic manipulations. We found daily variations in synaptic GABA release from AVP neurons, as well as from non-AVP neurons. Deficiency of AVP-neuronal GABA release increased the phase difference of morning and evening locomotor activities and caused the correspondent bimodal daily rhythm of SCN neuronal activities without significant desynchronization of molecular clocks in the SCN, but with altered phase relationships between the SCN molecular clocks and behavioral rhythms. Taken together, these findings suggest that GABAergic transmission of AVP neurons temporally confines behavior to the appropriate time window of SCN molecular clocks via the regulation of SCN neuronal activity (*SI Appendix*, Fig. S10). Thus far, the activity time, or association between morning and evening locomotor activity components, has been considered to be regulated by the phase distribution of multiple molecular clocks in individual SCN neurons, as exemplified by the dual oscillator model (43). However, the present study suggests that clock gene-based molecular clocks are necessary but not sufficient to appropriately shape the circadian rhythm, underscoring the importance of intercellular communications mediated by GABA. Thus, we propose an additional regulatory layer of circadian pattern formation on the molecular clocks in the SCN. Such a layered structure may partially resemble the central circadian pacemaker network of *Drosophila*, in which neuropeptide modulation is required to sequentially time outputs from a network of synchronous molecular pacemakers (47–49).

Materials and Methods

All experimental procedures involving animals were approved by the appropriate institutional animal care and use committees of Kanazawa University and Meiji University. All mice used in this study were generated by crossing previously described genotypes (14, 17, 18, 26, 34, 50). Slice electrophysiology, behavioral analyses, generation of AAV vectors, histological studies, PER2::LUC bioluminescence measurements, in vivo fiber photometry, and in vivo MUA recordings were performed as previously described (13, 14, 19, 29, 36, 51). More detailed information on materials and methods is described in *SI Appendix, Supplementary Materials and Methods*.

Data Availability. All study data are included in the article and supporting information.

ACKNOWLEDGMENTS. We thank S. Takamori for rat *Vgat* cDNA; K. Deisseroth for *pAAV-DIO-hChR2(H134R)-EYFP-WPRE-pA*; B. Roth for *pAAV-DIO-mCherry*; D. Kim and the GENIE Project for *pGP-AAV-CAG-FLEX-jGCaMP7s-WPRE*; B. Sabatini for *pAAV-Ef1a-DIO-EGFP-WPRE-pA*; the University of Pennsylvania Vector Core for *pAAV2-rh10*; H. Okamoto for technical support to generate *Avp-Cre* mouse; B. B. Lowell for the *Vgat*$^{flox/flox}$ mouse; D. R. Weaver for the *CK1δ*$^{flox/flox}$ mouse; H. Zeng for the Ai14 mouse; Z. J. Huang for the *Vip-ires-Cre* mouse; J. Takahashi for the *Per2::Luc* reporter mouse; and A. Matsui, M. Fukushi, and M. Kawabata for technical assistance. This study was supported in part by Ministry of Education, Culture, Sports, Science, and Technology/Japan Society for the Promotion of Science (MEXT/JSPS) KAKENHI Grants 15K21745, 16H05120, 18H04941, 18H04972, 19H03399, 20K21498; The Japan Agency for Medical Research and Development Wise; the Takeda Science Foundation; the Uehara Memorial Foundation; by the Yamada Science Foundation; the Japan Foundation for Applied Enzymology; the Daiichi Sankyo Foundation of Life Science; the Kao Research Council for the Study of Healthcare Science; the Kanazawa University CHOZEN project (M.M.); KAKENHI 18K06519 (to T.M.); and KAKENHI 19K21241, 20K07259 (to Y. Tsuno).

1. D. K. Welsh, J. S. Takahashi, S. A. Kay, Suprachiasmatic nucleus: Cell autonomy and network properties. *Annu. Rev. Physiol.* **72**, 551–577 (2010).
2. M. Brancaccio, A. P. Patton, J. E. Chesham, E. S. Maywood, M. H. Hastings, Astrocytes control circadian timekeeping in the suprachiasmatic nucleus via glutamatergic signaling. *Neuron* **93**, 1420–1435.e5 (2017).
3. S. J. Aton, C. S. Colwell, A. J. Harmar, J. Waschek, E. D. Herzog, Vasoactive intestinal polypeptide mediates circadian rhythmicity and synchrony in mammalian clock neurons. *Nat. Neurosci.* **8**, 476–483 (2005).
4. A. J. Harmar *et al.*, The VPAC(2) receptor is essential for circadian function in the mouse suprachiasmatic nuclei. *Cell* **109**, 497–508 (2002).
5. J.-D. Li, K. J. Burton, C. Zhang, S.-B. Hu, Q.-Y. Zhou, Vasopressin receptor V1a regulates circadian rhythms of locomotor activity and expression of clock-controlled genes in the suprachiasmatic nuclei. *Am. J. Physiol. Regul. Integr. Comp. Physiol.* **296**, R824–R830 (2009).
6. E. S. Maywood, J. E. Chesham, J. A. O'Brien, M. H. Hastings, A diversity of paracrine signals sustains molecular circadian cycling in suprachiasmatic nucleus circuits. *Proc. Natl. Acad. Sci. U.S.A.* **108**, 14306–14311 (2011).
7. D. Ono, S. Honma, K. Honma, Differential roles of AVP and VIP signaling in the postnatal changes of neural networks for coherent circadian rhythms in the SCN. *Sci. Adv.* **2**, e1600960 (2016).
8. D. Ono, K. I. Honma, Y. Yanagawa, A. Yamanaka, S. Honma, Role of GABA in the regulation of the central circadian clock of the suprachiasmatic nucleus. *J. Physiol. Sci.* **68**, 333–343 (2018).
9. C. Liu, S. M. Reppert, GABA synchronizes clock cells within the suprachiasmatic circadian clock. *Neuron* **25**, 123–128 (2000).
10. G. M. Freeman Jr, R. M. Krock, S. J. Aton, P. Thaben, E. D. Herzog, GABA networks destabilize genetic oscillations in the circadian pacemaker. *Neuron* **78**, 799–806 (2013).
11. H. Albus, M. J. Vansteensel, S. Michel, G. D. Block, J. H. Meijer, A GABAergic mechanism is necessary for coupling dissociable ventral and dorsal regional oscillators within the circadian clock. *Curr. Biol.* **15**, 886–893 (2005).
12. J. A. Evans, T. L. Leise, O. Castanon-Cervantes, A. J. Davidson, Dynamic interactions mediated by nonredundant signaling mechanisms couple circadian clock neurons. *Neuron* **80**, 973–983 (2013).
13. M. Mieda, H. Okamoto, T. Sakurai, Manipulating the cellular circadian period of arginine vasopressin neurons alters the behavioral circadian period. *Curr. Biol.* **26**, 2535–2542 (2016).
14. M. Mieda *et al.*, Cellular clocks in AVP neurons of the SCN are critical for interneuronal coupling regulating circadian behavior rhythm. *Neuron* **85**, 1103–1116 (2015).
15. S. M. Wojcik *et al.*, A shared vesicular carrier allows synaptic corelease of GABA and glycine. *Neuron* **50**, 575–587 (2006).
16. D. Ono, K. I. Honma, Y. Yanagawa, A. Yamanaka, S. Honma, GABA in the suprachiasmatic nucleus refines circadian output rhythms in mice. *Commun. Biol.* **2**, 232 (2019).
17. Q. Tong, C. P. Ye, J. E. Jones, J. K. Elmquist, B. B. Lowell, Synaptic release of GABA by AgRP neurons is required for normal regulation of energy balance. *Nat. Neurosci.* **11**, 998–1000 (2008).

18. L. Madisen *et al*., A robust and high-throughput Cre reporting and characterization system for the whole mouse brain. *Nat. Neurosci.* **13**, 133–140 (2010).
19. Y. Tsuneoka, H. Funato, Modified in situ hybridization chain reaction using short hairpin DNAs. *Front. Mol. Neurosci.* **13**, 75 (2020).
20. S. Varadarajan *et al*., Connectome of the suprachiasmatic nucleus: New evidence of the core-shell relationship. *Eneuro* **5**, ENEURO.0205-18.2018 (2018).
21. X. Jin *et al*., A molecular mechanism regulating rhythmic output from the suprachiasmatic circadian clock. *Cell* **96**, 57–68 (1999).
22. H. Tei *et al*., Circadian oscillation of a mammalian homologue of the Drosophila period gene. *Nature* **389**, 512–516 (1997).
23. Z. S. Sun *et al*., RIGUI, a putative mammalian ortholog of the Drosophila period gene. *Cell* **90**, 1003–1011 (1997).
24. C. S. Pittendrigh, S. Daan, A functional analysis of circadian pacemakers in nocturnal rodents V. Pacemaker structure: A clock for all seasons. *J. Comp. Physiol.* **106**, 333–355 (1976).
25. J. Schaap *et al*., Heterogeneity of rhythmic suprachiasmatic nucleus neurons: Implications for circadian waveform and photoperiodic encoding. *Proc. Natl. Acad. Sci. U.S.A.* **100**, 15994–15999 (2003).
26. S.-H. Yoo *et al*., PERIOD2:LUCIFERASE real-time reporting of circadian dynamics reveals persistent circadian oscillations in mouse peripheral tissues. *Proc. Natl. Acad. Sci. U.S.A.* **101**, 5339–5346 (2004).
27. R. Enoki *et al*., Topological specificity and hierarchical network of the circadian calcium rhythm in the suprachiasmatic nucleus. *Proc. Natl. Acad. Sci. U.S.A.* **109**, 21498–21503 (2012).
28. J. A. Evans, T. L. Leise, O. Castanon-Cervantes, A. J. Davidson, Intrinsic regulation of spatiotemporal organization within the suprachiasmatic nucleus. *PLoS One* **6**, e15869 (2011).
29. A. Inutsuka *et al*., The integrative role of orexin/hypocretin neurons in nociceptive perception and analgesic regulation. *Sci. Rep.* **6**, 29480 (2016).
30. M. Ikeda *et al*., Circadian dynamics of cytosolic and nuclear Ca^{2+} in single suprachiasmatic nucleus neurons. *Neuron* **38**, 253–263 (2003).
31. L. Mei *et al*., Long-term in vivo recording of circadian rhythms in brains of freely moving mice. *Proc. Natl. Acad. Sci. U.S.A.* **115**, 4276–4281 (2018).
32. J. R. Jones, T. Simon, L. Lones, E. D. Herzog, SCN VIP neurons are essential for normal light-mediated resetting of the circadian system. *J. Neurosci.* **38**, 7986–7995 (2018).
33. H. Dana *et al*., High-performance calcium sensors for imaging activity in neuronal populations and microcompartments. *Nat. Methods* **16**, 649–657 (2019).
34. H. Taniguchi *et al*., A resource of Cre driver lines for genetic targeting of GABAergic neurons in cerebral cortex. *Neuron* **71**, 995–1013 (2011).
35. S. T. Inouye, H. Kawamura, Persistence of circadian rhythmicity in a mammalian hypothalamic "island" containing the suprachiasmatic nucleus. *Proc. Natl. Acad. Sci. U.S.A.* **76**, 5962–5966 (1979).
36. T. J. Nakamura *et al*., Age-related decline in circadian output. *J. Neurosci.* **31**, 10201–10205 (2011).
37. W. Nakamura *et al*., In vivo monitoring of circadian timing in freely moving mice. *Curr. Biol.* **18**, 381–385 (2008).
38. J. Itri, C. S. Colwell, Regulation of inhibitory synaptic transmission by vasoactive intestinal peptide (VIP) in the mouse suprachiasmatic nucleus. *J. Neurophysiol.* **90**, 1589–1597 (2003).
39. J. Itri, S. Michel, J. A. Waschek, C. S. Colwell, Circadian rhythm in inhibitory synaptic transmission in the mouse suprachiasmatic nucleus. *J. Neurophysiol.* **92**, 311–319 (2004).
40. M. Perelis *et al*., Pancreatic β cell enhancers regulate rhythmic transcription of genes controlling insulin secretion. *Science* **350**, aac4250 (2015).
41. S. Wagner, M. Castel, H. Gainer, Y. Yarom, GABA in the mammalian suprachiasmatic nucleus and its role in diurnal rhythmicity. *Nature* **387**, 598–603 (1997).
42. S. Farajnia, T. L. E. van Westering, J. H. Meijer, S. Michel, Seasonal induction of GABAergic excitation in the central mammalian clock. *Proc. Natl. Acad. Sci. U.S.A.* **111**, 9627–9632 (2014).
43. C. Helfrich-Förster, Does the morning and evening oscillator model fit better for flies or mice? *J. Biol. Rhythms* **24**, 259–270 (2009).
44. W. J. Schwartz, R. J. Coleman, S. M. Reppert, A daily vasopressin rhythm in rat cerebrospinal fluid. *Brain Res.* **263**, 105–112 (1983).
45. R. Enoki *et al*., Synchronous circadian voltage rhythms with asynchronous calcium rhythms in the suprachiasmatic nucleus. *Proc. Natl. Acad. Sci. U.S.A.* **114**, E2476–E2485 (2017).
46. W. D. Todd *et al*., Suprachiasmatic VIP neurons are required for normal circadian rhythmicity and comprised of molecularly distinct subpopulations. *Nat. Commun.* **11**, 4410 (2020).
47. F. Guo, X. Chen, M. Rosbash, Temporal calcium profiling of specific circadian neurons in freely moving flies. *Proc. Natl. Acad. Sci. U.S.A.* **114**, E8780–E8787 (2017).
48. X. Liang, T. E. Holy, P. H. Taghert, A series of suppressive signals within the Drosophila circadian neural circuit generates sequential daily outputs. *Neuron* **94**, 1173–1189.e4 (2017).
49. X. Liang, T. E. Holy, P. H. Taghert, Synchronous Drosophila circadian pacemakers display nonsynchronous Ca2+ rhythms in vivo. *Science* **351**, 976–981 (2016).
50. J. P. Etchegaray *et al*., Casein kinase 1 delta regulates the pace of the mammalian circadian clock. *Mol. Cell. Biol.* **29**, 3853–3866 (2009).
51. E. Hasegawa *et al*., Serotonin neurons in the dorsal raphe mediate the anticataplectic action of orexin neurons by reducing amygdala activity. *Proc. Natl. Acad. Sci. U.S.A.* **114**, E3526–E3535 (2017).